

Mixing State of Size-Selected Submicrometer Particles in the Arctic in May and September 2012

Kihong Park,^{*,†} Gibaek Kim,[†] Jae-suk Kim,[†] Young-Jun Yoon,[‡] Hee-joo Cho,[†] and Johan Ström[§]

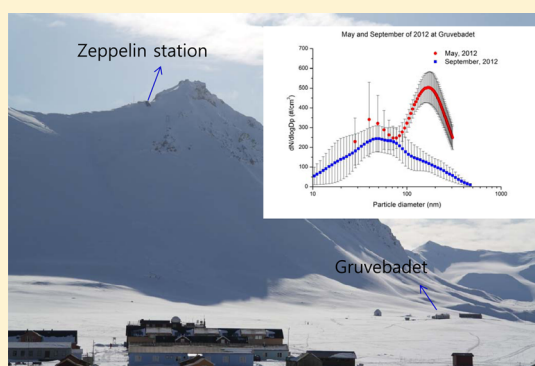
[†]National Leading Research Laboratory, School of Environmental Science and Engineering, Gwangju Institute of Science and Technology (GIST), 261 Cheomdan-Gwagiro, Buk-gu, Gwangju, 500-712, Republic of Korea

[‡]Korea Polar Research Institute, Get-pearl Tower, SongDo Techno Park, 12 Gaetbeal-ro, Yeonsu-Gu, Incheon, 406-840, Republic of Korea

[§]Department of Applied Environmental Science, Stockholm University, Svante Arrhenius väg 8, Stockholm, SE-11418, Sweden

S Supporting Information

ABSTRACT: Aerosols have been associated with large uncertainties in estimates of the radiation budget and cloud formation processes in the Arctic. This paper reports the results of a study of in situ measurements of hygroscopicity, fraction of volatile species, mixing state, and off-line morphological and elemental analysis of Aitken and accumulation mode particles in the Arctic (Ny-Ålesund, Svalbard) in May and September 2012. The accumulation mode particles were more abundant in May than in September. This difference was due to more air mass flow from lower latitude continental areas, weaker vertical mixing, and less wet scavenging in May than in September, which may have led to a higher amount of long-range transport aerosols entering the Arctic in the spring. The Aitken mode particles observed intermittently in May were produced by nucleation, absent significant external mixing, whereas the accumulation mode particles displayed significant external mixing. The occurrence of an external mixing state was observed more often in May than in September and more often in accumulation mode particles than in Aitken mode particles, and it was associated more with continental air masses (Siberian) than with other air masses. The external mixing of the accumulation mode particles in May may have been caused by multiple sources (i.e., long-range transport aerosols with aging and marine aerosols). These groups of externally mixed particles were subdivided into different mixing structures (internal mixtures of predominantly sulfates and volatile organics without nonvolatile species and internal mixtures of sulfates and nonvolatile components, such as sea salts, minerals, and soot). The variations in the mixing states and chemical species of the Arctic aerosols in terms of their sizes, air masses, and seasons suggest that the continuous size-dependent measurements observed in this study are useful for obtaining better estimates of the effects of these aerosols on climate change.



INTRODUCTION

The Arctic is a key region of the Earth that is highly sensitive to small environmental changes in the Earth's climate due to its complex feedback system.¹ The largest increase in annual mean temperature has been observed in the Arctic, where the warming rate during the last century was nearly two times higher than the rate measured in the rest of the world. This warming suggests that climate change in Arctic regions may be considered a predictor of climate change on a global scale.^{1–3} Several explanations have been offered for this amplification: the global increase in greenhouse gas concentrations or changes in the Arctic ozone budget^{3,4} and transport of anthropogenic light-absorbing carbonaceous particles from lower latitudes.^{3,5–9} Typically, aerosols play a critical role in the radiation balance by scattering and/or absorbing incoming solar light (direct climate forcing) and in cloud formation processes by acting as cloud condensation nuclei (CCN) (indirect climate forcing). These effects depend on details, such as the size, mixing state, and chemical constituents of the particles.^{10–14}

Both optical (light scattering and light absorption efficiency) and hygroscopic (an effective indicator of CCN development) properties of particles can vary with their mixing state.

Anthropogenic aerosols have been observed in the Arctic atmosphere and its snow and ice.^{1,3,15–20} The high aerosol mass loading in the Arctic has often been observed in the spring, leading to a reduction of visibility known as the Arctic haze. It has been reported that this Arctic haze is caused by anthropogenic aerosols transported from the lower latitude continents (e.g., northern Eurasia)^{21–28} and is most often observed in the late winter and early spring, though not often in summer.^{16,29–31} The cold and dry conditions in the late winter and spring suppress wet deposition and vertical mixing, which favor the accumulation of transported pollutants in the Arctic

Received: April 29, 2013

Revised: December 10, 2013

Accepted: December 11, 2013

Published: December 11, 2013

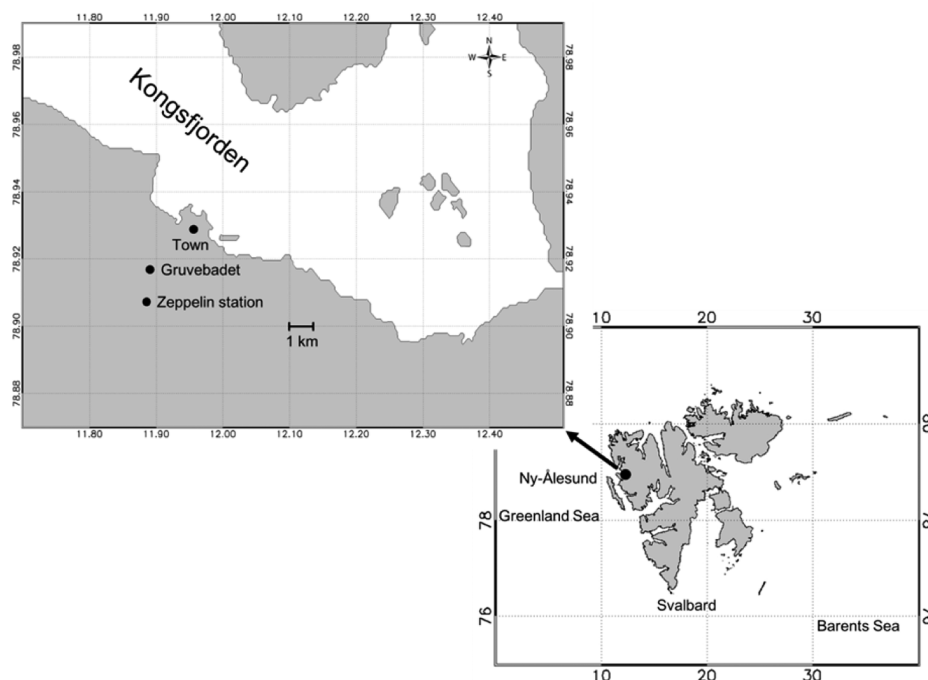


Figure 1. Map of sampling sites (Ny-Ålesund (78.6° N, 11.6° E)).

atmosphere.³² Earlier research²⁶ has shown that combustion sources accounted for significant organic components in the submicrometer range in the springtime Arctic haze over the Arctic parts of the Atlantic and Pacific oceans. Biomass burning is also known to be an episodic potential source of anthropogenic aerosols in the Arctic (e.g., black carbon in the air and in snow or ice),^{5,33} which play an important role in the radiative budget in the Arctic. In general, less transport of contaminants to the Arctic and fewer residential heating events in the source regions together with stronger vertical mixing and wet scavenging in the Arctic lead to cleaner air in the summer than in the spring.³⁴ It has been reported that the aerosols experience a highly rapid transition in their size distribution between the spring and summer, primarily due to changes in their air mass origins but also from photochemical production of new particles (this transition occurs over a period of approximately two weeks every year).^{16,29–31} A combination of the transport patterns of the air mass and the strength of the aerosol sources and sinks can influence the rapid change in the properties of Arctic aerosols between the spring and summer.^{16,24,31,35} In addition to anthropogenic aerosols transported from continents at lower latitudes, marine aerosols emitted by the oceans can contribute to a large portion of the Arctic aerosols (e.g., sea salts, biogenic organic aerosols). The extent of Arctic sea ice has decreased during the last few decades, leading to the increasing importance of the marine influence on Arctic aerosols.³⁶

Although previous studies have provided useful information regarding the characteristics of the Arctic aerosols, measurements of the particle number size distribution and/or noncontinuous measurements of the chemical/morphological properties of the particles is insufficient for a complete understanding of the sources and formation pathways of the Arctic aerosols or for estimating their effects on climate change. In this study, in situ measurements of the size-dependent hygroscopicity (water affinity), volatility (volatile particles), and mixing state of the Arctic aerosols and measurements of their

particle size distribution were conducted during the transition from spring to summer (May 2012) and in September 2012. May was selected because a rapid change in the size distribution has been observed with weakening of the Arctic haze in May (this transition has occurred over a period of approximately two weeks every year),³⁰ providing a good opportunity to understand the rapid transition of aerosol properties from spring to summer. In September 2012, the Arctic atmosphere was very clean (the lowest particle number concentration was observed in the fall during the period of March 2000 to March 2010³⁷), and a large area of open ocean was available due to melting of sea ice. A comparison between the aerosol properties in May and September will also provide useful information regarding the aerosol's source and formation in the Arctic atmosphere during various seasons, although two 15-day data sets (hygroscopicity, volatility, and mixing state data) in May and September are not fully representative of each corresponding season. The particle number size distributions were measured using a combination of a differential mobility analyzer (DMA) and a condensation particle counter (CPC) at the Gruvebadet and Zeppelin stations at elevations of 61 and 474 m above sea level, respectively. Both stations are located near Ny-Ålesund (78.6° N, 11.6° E), Svalbard. The measurements of the hygroscopicity and volatility of particles of selected sizes (Aitkin mode and accumulation mode) were performed at Gruvebadet using the hygroscopicity and volatility tandem differential mobility analyzer (HVTDMA) technique, a method that is capable of providing important information regarding the composition and mixing state (external and internal mixing) of the particles.^{38–40} The hygroscopicity of the particles provided information relevant to the water uptake and the particle effectiveness as a CCN, which influences the microphysical and optical properties of the clouds. The measurements of volatility were conducted at 100 °C, at which sulfates or other salts are not evaporated, whereas most of the volatile organics are evaporated (i.e., compounds more volatile than ammonium sulfate), making it possible to identify

the presence of volatile organic species and determine their component fractions. The effects of the transport pathways of air masses were examined using an air-mass backward trajectory analysis. In addition, off-line morphological and elemental analyses of particles were conducted using transmission electron microscopy (TEM)/energy dispersive spectroscopy (EDS) to provide supporting information regarding the morphology and mixing state of the particles.

MATERIALS AND METHODS

The measurements were made at Ny-Ålesund (78.6° N, 11.6° E), Svalbard Islands (Figure 1). Ny-Ålesund is the location of many cooperative international projects for the study of the Arctic environment and ecosystem. The Kongsvegen glacier is located approximately 10 km east of Ny-Ålesund. The Kongsfjorden, where Ny-Ålesund is located, can often be frozen during the winter such that Ny-Ålesund has a continental climate in winter and a coastal climate in summer. The mean air temperature at Ny-Ålesund during the period 1961–1990 was approximately −15 °C in February, −5 °C in May, 3 °C in August, 0 °C in September, and −10 °C in November. As shown in Figure 1, the Gruvebadet station is located approximately 1.5 km south of and approximately 50 m higher than the small town of Ny-Ålesund (11 m above sea level). The Zeppelin station is located on the ridge of Zeppelin Mountain, approximately 2.3 km south of the town of Ny-Ålesund and 474 m above sea level. The particle number size distribution measurements were performed at two locations (Gruvebadet and Zeppelin) at elevations of 61 and 474 m above sea level, respectively, and all of the other aerosol measurements were conducted at Gruvebadet.

The ambient samples were drawn through an inlet tube with an inner diameter of 100 mm from a height of 5 m above the ground at a flow rate of 150 Lpm. The sampled aerosols passing through the inlet tube were subsequently split for delivery into each aerosol instrument. Before they were introduced into the aerosol measurement system, the atmospheric particles were first dried to 10–15% RH using a series of diffusion driers. Continuous measurements of the size distributions (3–85 nm and 25–800 nm) were measured at Zeppelin in May 2012 using a differential mobility particle sizer (DMPS), which consists of a differential mobility analyzer (DMA) and a condensation particle counter (CPC). At Gruvebadet, the size distributions (20–306 nm and 10–470 nm) were measured using the DMPS in May and September 2012. The HVTDMA system was used for measuring the hygroscopicity and volatility of the size-selected particles. The HVTDMA system primarily consisted of two DMAs, a heated tube, a humidifier, and a CPC (TSI 3010, USA). Particles of a given size were selected in the first DMA and directed into a heated tube or humidifier for subsequent sizing in the second DMA and CPC. This yielded data regarding the change in particle size after heating to ~100 °C or humidifying to an RH of ~85%. This measurement system provided the hygroscopic growth factor (HGF) and shrinkage factor (SF) at a given RH and heater temperature, respectively. The HGF is the ratio of the particle mobility diameter at an elevated RH to that under dry conditions (10–15% RH), and the SF is the ratio of the particle mobility diameter at an elevated temperature (100 °C) relative to that at room temperature (~25 °C). At a heater temperature of 100 °C, organic carbon species can be considered candidate volatile species because ammonium sulfate or other inorganic species (e.g., salts) are not volatile at that temperature, and water is

removed from the particles before they enter the tandem measurement system. If the size-selected particles were present in an external mixing state, two or more hygroscopic or volatile groups of particles were expected to appear under conditions of increased RH or T, respectively. In addition, the heater temperature was occasionally increased to 250 °C to identify the presence of nonvolatile species in internally mixed particles. If the particles were completely evaporated, then no particles were detected at 250 °C, which is the case for ammonium sulfate, ammonium nitrate, sulfuric acid, C24–C32, and dicarboxylic acids, based on laboratory measurements.⁴⁰ If particles were present after the removal of the volatile species at 250 °C, then they likely were nonvolatile species (e.g., sodium chloride, black carbon (BC), or mineral particles).

To determine the morphology and elemental composition of individual particles, the particles were collected on a TEM grid. These samples were subsequently analyzed using TEM (200-kV accelerating voltage and 100- μ A beam current) (JEOL JEM-2100F) and energy dispersive spectroscopy (EDS) (OXFORD INCAx-sight). The transport patterns of the air masses during the sampling periods were determined using air-mass backward trajectory data (<http://www.arl.noaa.gov/ready/hysplit4.html>). A 120- or 240-h air-mass backward trajectory analysis was performed below heights of 500 m above the ground at the sampling site (78.6° N, 11.6° E). Additionally, the mass concentration measured in the Arctic was related to the air mass trajectories to better understand how the various source regions affect the aerosol concentrations in the Arctic.³⁷ The mass concentration was calculated from the number size distribution data assuming spherical particles with a density of 1 g/cm³. The concentration measured at the sampling site was assigned to the grids in the path of the air mass trajectory, and the concentration was normalized by the number of trajectories crossing the specific grid. This analysis provided a measure of the particle concentration at the sampling site after the air mass trajectory passed over the grids.³⁷

RESULTS AND DISCUSSION

Comparison between Size Distribution Data of May and September. The average size distributions in May and September 2012 are compared in Figure 2a. A significant difference in the size distribution was observed. The number concentration of submicrometer particles was significantly higher in May than in September. The accumulation mode particles were dominant in May, which may be related to long-range transport of aerosols from anthropogenic sources.^{30,31} Because May is during the transition from spring to summer, the Aitken mode particles (which were reportedly dominant in summer) appeared occasionally. The Aitken mode particles have been reported as related to production of new particles via nucleation.³¹ In summer, it was observed that the accumulation mode particles were suppressed, whereas the Aitken mode particles became significant. The smaller number of accumulation mode particles in the summer may have occurred due to weakening of the long-range transport aerosols with the change of air masses and strong wet removal during the summer. However, it was reported that a few long-range transport events (e.g., forest fires) also occurred in the Arctic in the summer.⁴¹ The high concentration of the Aitken mode particles in May was caused by increased photochemical activity and a weak condensational sink effect (i.e., few accumulation mode particles) leading to new particle formation.³⁷ In September, the concentrations of both Aitken and accumulation mode

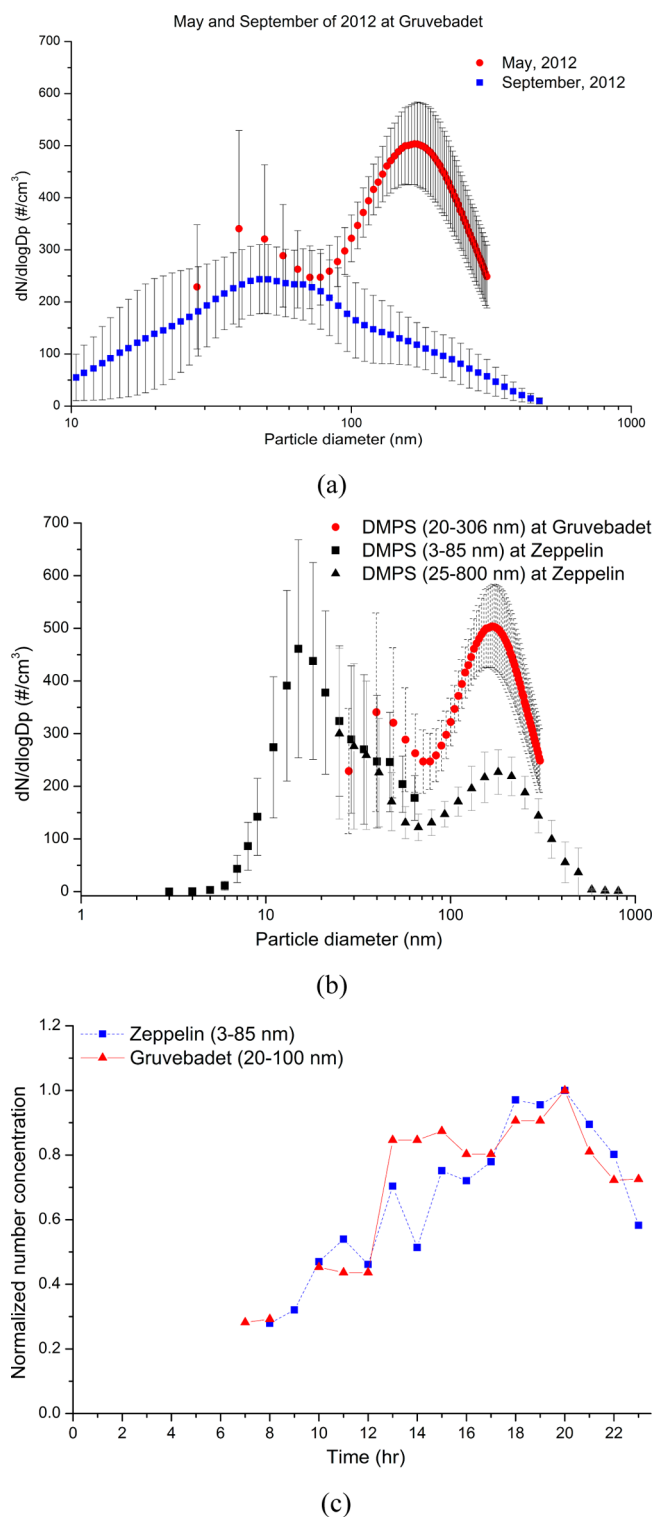


Figure 2. (a) Average size distributions at Gruvebadet in May and September 2012, (b) average size distributions at two locations (Gruvebadet and Zeppelin) in May 2012 (the error bar represents standard deviation), and (c) diurnal variations of normalized number concentrations by peak concentration at Gruvebadet and Zeppelin on 5/4/2012.

particles decreased, as shown in Figure 2a. The intensified wet removal in September (the highest precipitation occurred in the months of August and September during the period of 2000–2010)³⁷ along with the weakening of the long-range transport

aerosols may have contributed to the smaller number of Aitken and accumulation mode particles. Although there is a larger area of open ocean in September than May, the stronger wet removal process may also have led to particle removal, including removal of particles originating from the ocean. The low concentration of particles in September is consistent with the earlier observation by others that the annual minimum in the total aerosol number concentration occurred in September or October, based on the 10 years of aerosol number size distribution data.³⁷

Comparison between Size Distribution Data from Gruvebadet and Zeppelin. A comparison of the average size distributions at two locations (Gruvebadet and Zeppelin, located ~500 m from each other at elevations of 61 and 474 m above sea level, respectively) was performed in May 2012; the results are shown in Figure 2b. Note that any data associated with winds passing through the nearby town were removed to minimize local anthropogenic emissions. Because the two size distributions do not cover exactly the same size range, a direct comparison of the two data sets from the two sites is difficult. The characteristics of the Aitken mode particles were comparable, whereas the amount of the accumulation mode particles was smaller at Zeppelin than at Gruvebadet. The smaller accumulation mode particles at Zeppelin may have been due to more dilution by vertical mixing and more wet removal at the higher elevation.³¹ Although the elevations of the sampling locations differ by ~410 m and the sites are ~1 km apart, the Aitken mode particles appeared nearly simultaneously at both locations, suggesting that they were locally produced via nucleation over an area exceeding several kilometers across. For example, the diurnal variations in the normalized number concentrations at Gruvebadet and Zeppelin on 5/4/2012 are shown in Figure 2c. The Aitken mode particles increased with increasing solar intensity at approximately 12:00 and decreased after 20:00 at both sites, suggesting that photochemical activity played an important role in the formation of the Aitken mode particles. Bubbles bursting in the ocean and melting of Siberian tundra may provide precursor materials responsible for new particle formation.^{16,42} Vertical mixing of upper and lower air can provide conditions favorable for the production of new particles.⁴³ Additional measurements of hygroscopicity and volatility of the Aitken and accumulation mode particles should improve our understanding of their sources and formation pathways and will be discussed in the next section.

Hygroscopicity, Volatility, and Mixing State. The hygroscopicity, volatility, and mixing state of the Aitken (~50 nm) and accumulation mode particles (~130 nm) were measured using the HVTDMA system at Gruvebadet. Figure 3 shows their HGF, SF, and mixing states when a new particle formation event (5/4/2012) was observed in the afternoon. During the period of enhanced concentration of the Aitken mode particles, the HGF and SF of the Aitken mode particles were 1.46 and 0.88, respectively, with no external mixing of various hygroscopic or volatile particle groups. The presence of volatile species and the observed HGF without external mixing suggest that these particles have the characteristic of an internal mixture of sulfate and volatile organic species. Note that pure ammonium sulfate and other inorganic salts are not evaporated at this temperature (100 °C). The data suggest that biogenic organic compounds in addition to sulfate may contribute to the Aitken mode particles via photochemical production, and that other particle source contributions to the Aitken mode particles were not significant. Other researchers^{44,45} reported that in the

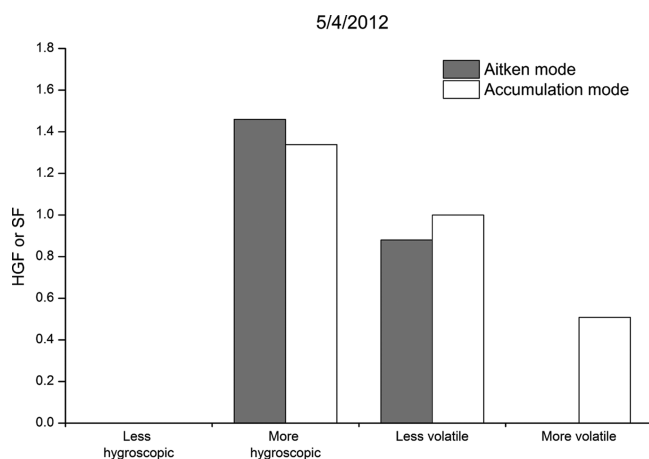
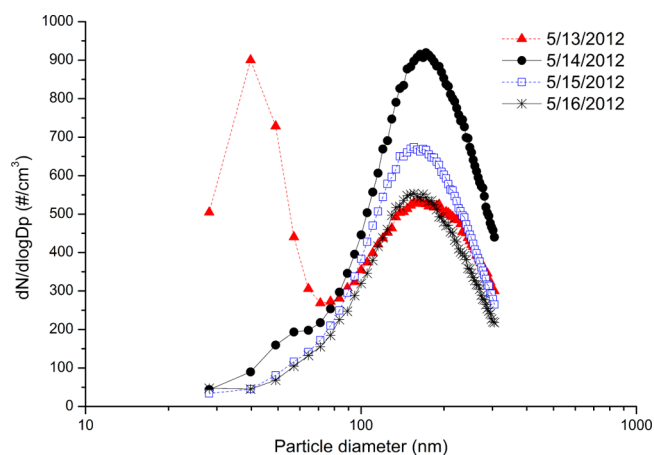


Figure 3. HGF, SF, and external mixing state of the Aitken (~ 50 nm) and accumulation mode particles (~ 130 nm) measured using the HVTDMA system at Gruevbadet when a new particle formation event (5/4/2012) occurred.

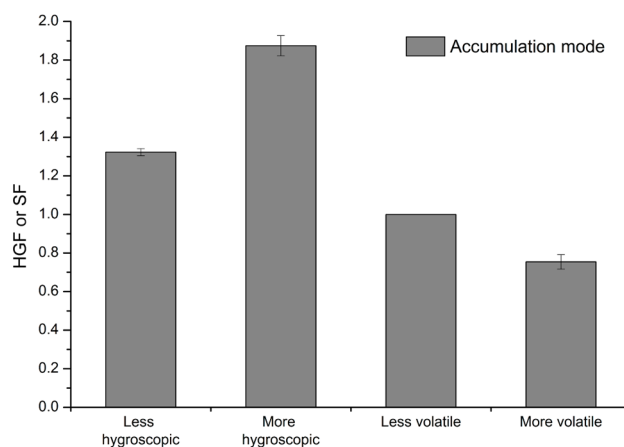
notably clean polar air masses, the organic compounds responsible for particle formation and growth are primarily of biogenic origin. The accumulation mode particles were observed to be externally mixed with various volatile species (i.e., an external mixture of pure sulfate (SF = 1.00) and volatile organics (SF = 0.51)), suggesting that multiple sources contributed to the accumulation mode particles.

On 5/14/2012, 5/15/2012, and 5/16/2012, the accumulation mode particles became dominant over the Aitken mode, as shown in Figure 4a. For comparison, the size distribution on 5/13/2012 (when the Aitken mode was dominant) was included in Figure 4a. Due to the increase in the accumulation mode particles during this period, the production of the Aitken mode particles was suppressed (i.e., the accumulation mode particles may have acted as a sink for precursors responsible for the Aitken mode particles).³⁷ The average values of HGF, SF, and the mixing state of the accumulation mode particles over the 3 days are shown in Figure 4b. These particles were externally mixed with various hygroscopic and volatile particle groups similar to the observation on 5/4/2012, discussed in the previous section. Particles with an HGF of 1.87 and an SF of 1.00 can be related to sulfate and aged sea salt species (highly hygroscopic and nonvolatile), whereas particles with an HGF of 1.32 and an SF of 0.75 may be a mixture of sulfate and volatile organics. The presence of external mixing groups of the accumulation mode particles may have been caused by both long-range transport aerosols with aging and aerosols originated from ocean. It was previously reported that this external mixing is abundant under Arctic haze conditions with increasing aerosol loadings and that internal mixing is dominant during background conditions.⁴⁶ Typically, in the winter and spring, Arctic fronts proceed south, making it easier for air contaminants to be transported to the Arctic, whereas in the summer and fall, Arctic fronts prevent long-range transport of contaminants from Europe and Russia.²⁸ In our study, the lowest HGF of submicrometer particles in May 2012 was 1.16. The HGF and SF of fresh soot or black carbon particles are generally known to be 1.0 and 1.0, respectively.⁴⁰ Thus, any soot particles, if present, may have aged and become hygroscopic during their long-range transport.

The hygroscopicity, volatility, and external mixing state of the Aitken (~ 50 nm) and accumulation mode particles (~ 130 nm)



(a)



(b)

Figure 4. (a) Size distributions on 5/13/2012, 5/14/2012, 5/15/2012, and 5/16/2012, and (b) average values of HGF, SF, and external mixing state of the accumulation mode particles on 5/14/2012, 5/15/2012, and 5/16/2012.

in May and September 2012 are summarized in Figure 5. Previous studies reported that the transition in the aerosol size distribution from spring to summer could not be explained by transport alone, although a seasonal flow pattern existed.^{3,17,28,47} The accumulation mode particles in May were significantly externally mixed with different hygroscopic species compared with those in September. Both long-range transport and marine aerosols may have contributed to the external mixing of the accumulation mode particles in May. Less external mixing with different hygroscopic species was observed in September. Changes in the transport pathways (less aerosol transport from low latitudes),¹⁷ enhanced vertical mixing due to solar heating,⁴⁸ and an increase in wet scavenging contributed to the smaller number and less external mixing of the accumulation mode particles in September. The average HGFs of the 50-nm and 130-nm particles in May were 1.41 and 1.33 (1.87 for “more hygroscopic” particles), respectively, whereas these values were 1.21 and 1.22, respectively, in September. The average SFs of the 50-nm and 130-nm particles in May were 0.98 (0.65 for “more volatile” particles) and 1.00 (0.66 for “more volatile” particles), respectively, whereas these values were 0.93 (0.71 for “more volatile” particles) and 0.94 (0.61 for “more volatile” particles), respectively, in September.

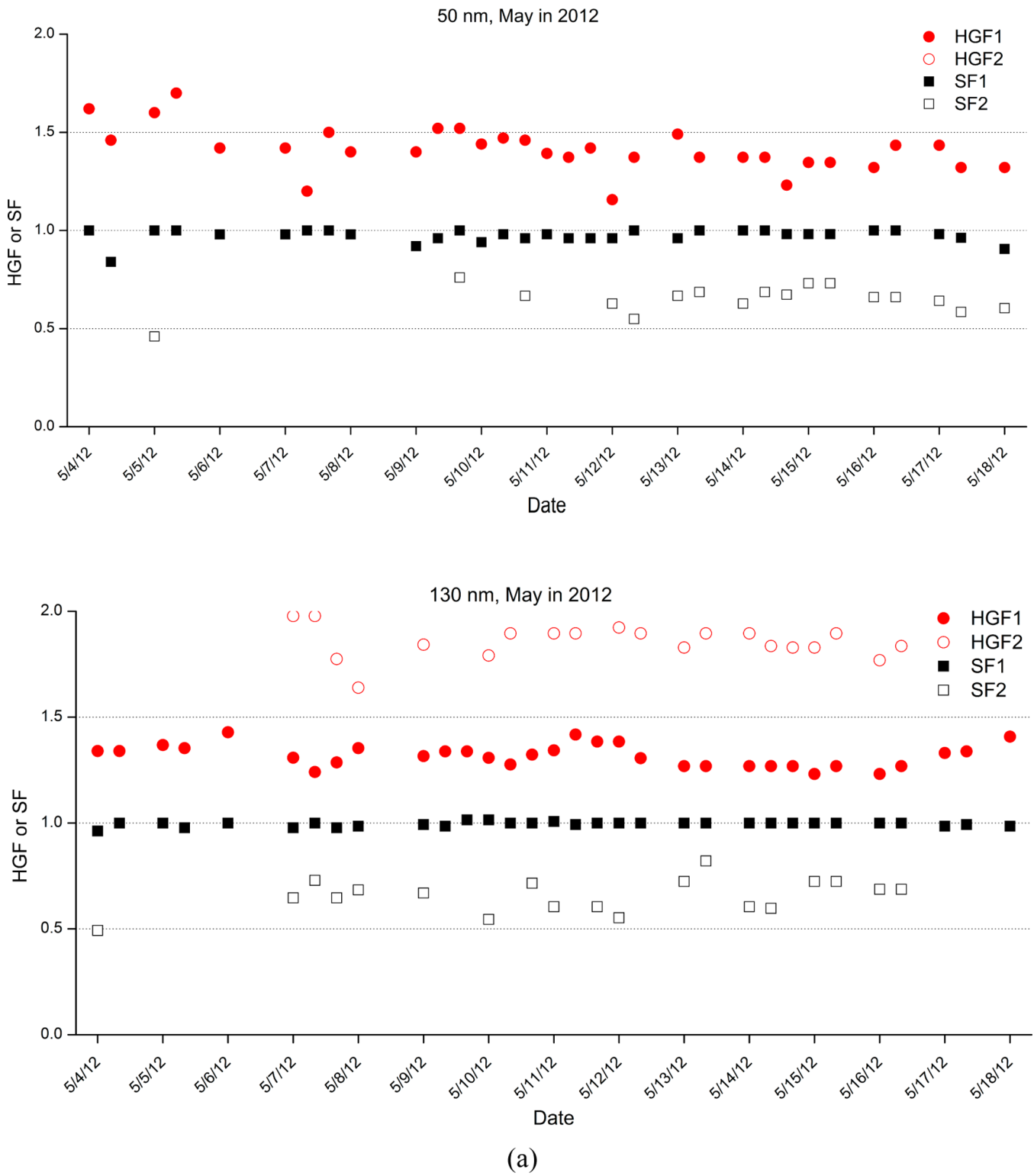
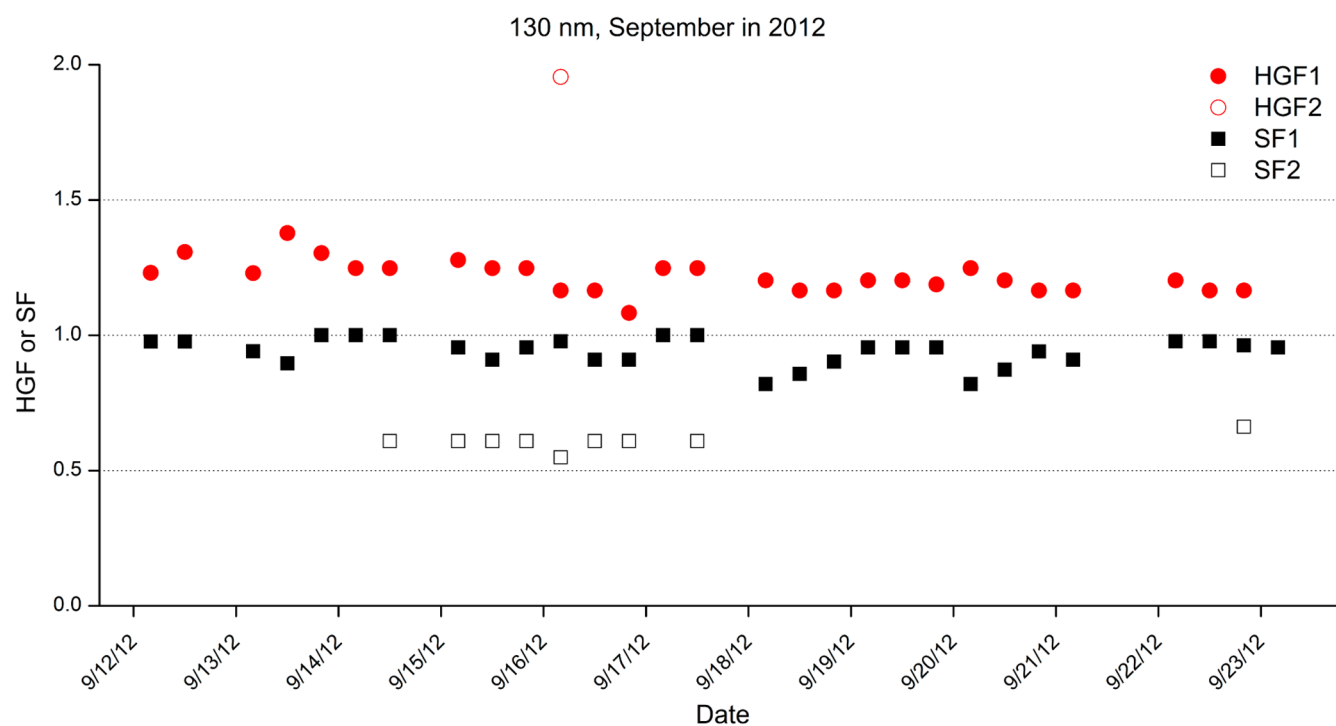
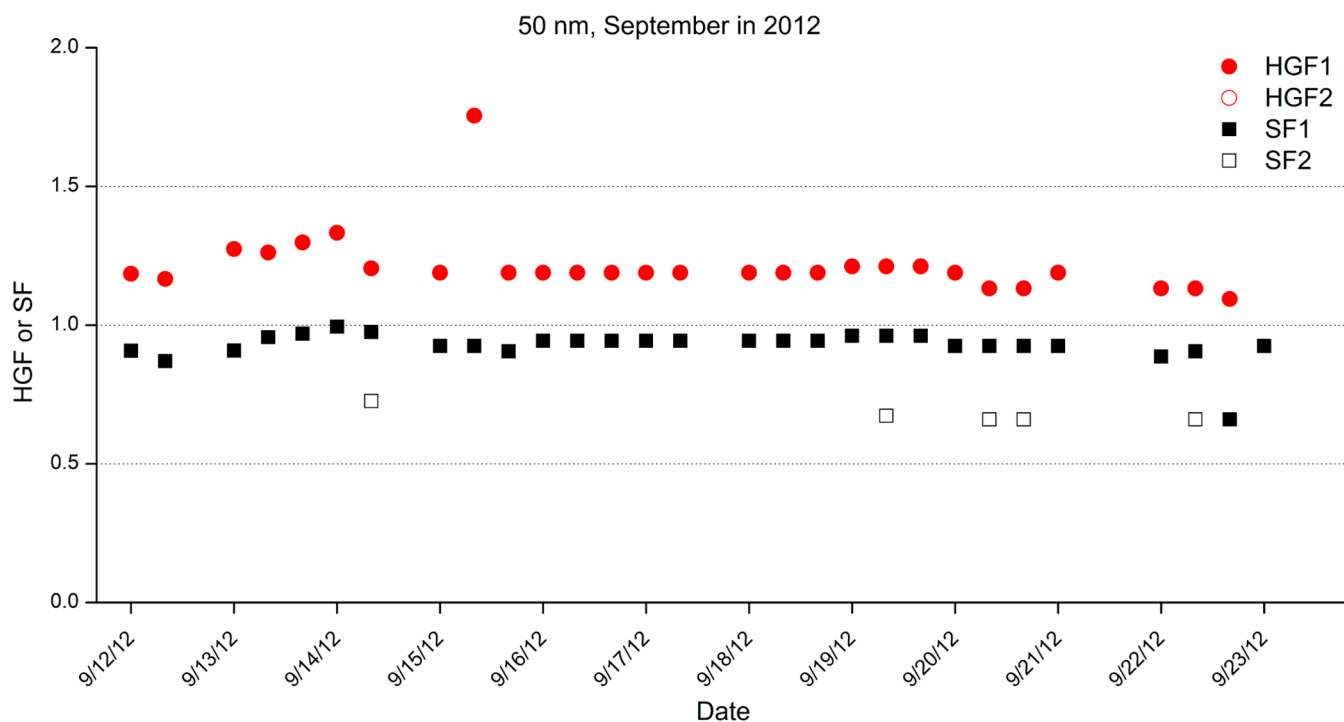


Figure 5. continued



(b)

Figure 5. Variations in HGF (HGF1 for “less-hygroscopic” particles and HGF2 for “more-hygroscopic” particles), SF (SF1 for “less-volatile” particles and SF2 for “more-volatile” particles), and external mixing state of the Aitken (~ 50 nm) and accumulation mode particles (~ 130 nm) in (a) May 2012 and (b) September 2012.

The data suggest that the submicrometer particles in September were somewhat less hygroscopic and more volatile than those in May (i.e., they contained a higher amount of volatile and less hygroscopic species in individual particles). Although the number of particles was smaller in September than in May,

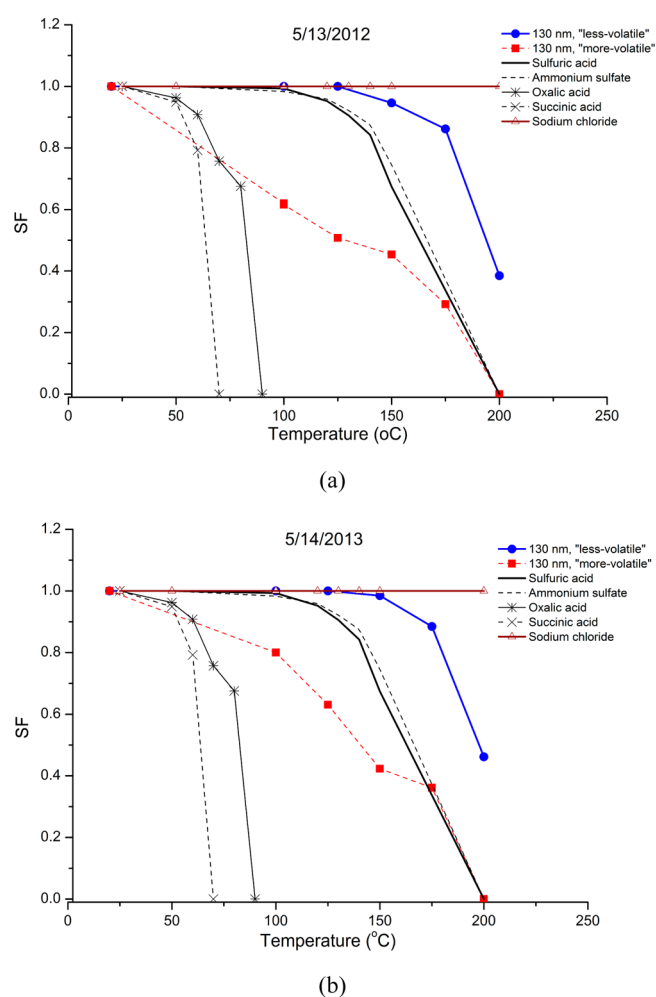
the additional marine source exposure due to ice melting may have led to a greater availability of biogenic organic compounds from the ocean, contributing to the higher SF, and the preferential wet removal of more hygroscopic particles may have contributed to the lower HGF in September.

Table 1. Average Mass Concentration, HGF, SF, and External Mixing State of Accumulation Mode Particles (130 nm) Associated with Various Air Masses in May 2012

air mass origin	date	mass concentration ($\mu\text{g}/\text{m}^3$)	HGF1	HGF2	SF1	SF2	percentage of occurrence when external mixing of various hygroscopic species was observed	percentage of occurrence when external mixing of various volatile species was observed
Siberia	5/4/2012, 5/5/2012, 5/6/2012, 5/7/2012, 5/8/2012, 5/11/2012, 5/12/2012, 5/13/2012, 5/14/2012	0.59	1.34	1.87	0.99	0.62	75	63
Northern Europe	5/17/2012, 5/18/2012	0.27	1.25	1.81	0.99	0.69	100	100
Northern Greenland	5/9/2012	0.39	1.33	1.84	0.99	0.67	33	33
The Arctic Ocean	5/10/2012, 5/15/2012, 5/16/2012	0.41	1.27	1.85	1.00	0.68	57	57

Effect of Air Mass Transport. By using air-mass backward trajectory analysis, we investigated the manner in which various source areas and air mass transport potentially influenced the aerosol properties observed in the Arctic. Others have reported that in the spring (March, April, and May), a majority of air mass trajectories over the Arctic Ocean were from Alaska, Siberia, and Eurasia, there was a minimum influence of air mass transport over the Atlantic Ocean based on air mass data during the 10-year period, and the air mass pattern changed in the summer, with a much larger portion of the air mass coming from the northern Atlantic Ocean.³⁷ A similar air mass pattern was observed in our study. The average mass concentration, HGF, SF, and external mixing state of the accumulation mode particles associated with various air masses in May 2012 were examined, as summarized in Table 1. We classified the air mass trajectories in May as air masses from Siberia, northern Europe, northern Greenland, and the Arctic Ocean. The average trajectory of each air mass group is shown in Figure S1(a) (Supporting Information (SI)). It was found that the mass concentration was the highest and an external mixing state was observed more often in the air mass from Siberia, suggesting that the long-range transported aerosols from continent significantly contributed to the accumulation mode particles as an external mixture in May. However, in September, the mass concentration and external mixing state of the accumulation mode particles displayed no dependence on the air mass pattern. To further investigate this difference, we correlated all air mass trajectories from various source regions in May and September to actual mass concentrations at the sampling site. As shown in SI Figure S1(b), the high mass concentration in May was clearly observed at the sampling site when the air mass originated in Siberia. However, in September, the air mass from Siberia was not clearly correlated to the high concentration at the receptor, and the concentration was low, regardless of the air mass trajectories. This pattern suggests that the similar air mass patterns during these two particular months did not lead to similar aerosol characteristics. The strong wet scavenging mechanism in September played an important role in removing the accumulation mode particles and hindering the effective transport of continental aerosols into the Arctic (the highest precipitation in the Arctic typically occurs in August and September³⁷).

Presence of Nonvolatile Cores in the Accumulation Mode Particles. When the air masses came from a continental area, the mixing structure of the accumulation mode particles was examined in more detail by gradually increasing the heater temperature up to 200 °C in the HVTDMA system, as shown in Figure 6. For comparison, the evaporative behaviors of

**Figure 6.** SF of the accumulation mode particles associated with air masses from Russia as a function of heater temperature on (a) 5/13/2012 and (b) 5/14/2012.

laboratory-generated sodium chloride, sulfuric acid, ammonium sulfate, oxalic acid, and succinic acid of similar sizes were included. As shown in Figure 6, sodium chloride particles are nonvolatile, sulfuric acid and ammonium sulfate particles are less volatile, and dicarboxylic acids are highly volatile (*n*-alkanes are also highly volatile but are not shown). The accumulation mode particles were externally mixed with various volatile groups on 5/13/2012 and 5/14/2012. On both days, the “more volatile” particles such as ammonium sulfate completely evaporated when the heater temperature was increased to

200 °C, and a certain amount of species of the “more volatile” particles evaporated below 100 °C (note that ammonium sulfate and sulfuric acid particles did not evaporate below 100 °C). This observation suggests that the “more volatile” particles may consist of an internal mixture of sulfate and volatile organics lacking any nonvolatile core. In contrast, the “less volatile” particles started to evaporate above 100 °C but were not completely evaporated at 200 °C, unlike the “more volatile” particles, suggesting that the “less volatile” particles consisted of sulfates and nonvolatile components such as sea salts, minerals, and soot. The mineral components (e.g., silicates and metallic components) may have originated from windblown dust and anthropogenic high-temperature processes. The data suggest that the accumulation mode particles were present in different mixing structures with and without nonvolatile cores due to their multiple sources and the aging process.

Morphology and Elemental Composition. Off-line morphological and elemental analyses of submicrometer particles (<200–300 nm) were also performed using TEM/EDS. A previous study²⁸ reported that sea salt, aged sea salt, silicates, and mixed particles (mixtures of sea salt, silicates, and Ca sulfates) are the most abundant particle groups in the coarse fraction (>500 nm), whereas the secondary aerosols, mixtures of sea salt, silicates, and Ca sulfates, and secondary aerosols with soot inclusion are most abundant in the fine fraction (<500 nm). In this study, particles much smaller (<200–300 nm) than those in previous works^{1,28} were examined. Based on the detected major elements and morphology, several distinct types of submicrometer particles were identified, but quantification of such particles associated with varying air masses and seasons was not conducted. The most abundant particle groups in this size range (<200–300 nm) were classified as organics (C and O) (SI Figure S2(a)), mixtures of organics and sulfate (C, O, and S) (Figure S2(b)), soot (C and O with agglomerated shape) (Figure S2(c)), aged sea salts (Na and Si/K/Mg/Cl) (Figure S2(d)), and mineral dust particles (Si/Al/Fe/Ti/Ca) (Figure S3). The organics–sulfate mixture and aged sea salts contributed to the hygroscopic species, whereas the organics contributed to the volatile species observed in the HVTDMA analyses. As shown in SI Figure S2(b), both particles consisted of mixtures of organics and sulfate, but they displayed different C/S ratios and morphologies. Particles with a high C/S ratio were more vulnerable to electron beam bombardment under high magnification (i.e., high electron beam energy), suggesting that they contained volatile species corresponding to particle groups with a high SF. Figure S2(c) shows soot particles with agglomerated shapes. Their compact shape and absence of particles with an HGF of 1.0 suggest that most of the soot particles may have been aged during their long-range transport. Figure S2(d) shows the aged sea salt particles. Due to their highly hygroscopic behavior, evidence of water in the particles was often observed in the TEM images. Particles with mineral dust components are shown in Figure S3. Various shapes (e.g., spherical, irregular, rod-shaped, aggregate) were observed in this group of particles. The mineral components (including metallic species) may have originated from windblown dust and high-temperature anthropogenic processes. These mineral components were responsible for the less volatile or nonvolatile components in the HVTDMA measurements. Aging of these particles cannot be identified from the TEM data, but the HVTDMA measurements suggest that a subset of these particles may also have aged and become hygroscopic.

Although not presented in this paper, a few P-containing particles that may have originated from biological materials were also observed.

This paper describes in situ measurements of the hygroscopicity, the fraction of volatile species, and the mixing state of submicrometer particles in the Arctic (Ny-Ålesund, Svalbard) in May and September 2012. A higher concentration of accumulation mode particles in May than in September was observed. This observation was due to more air mass flow from lower latitude continental areas, weaker vertical mixing, and less wet scavenging in May than in September, which may have led to the accumulation of the higher amount of long-range transport aerosols entering the Arctic in the spring. Additionally, external mixing was observed more often in May than in September, more often in accumulation mode particles than in Aitken mode particles, and more often in association with continental air masses (Siberian) than in association with other air masses. The external mixing of the accumulation mode particles in May may have been caused by multiple sources (i.e., long-range transport aerosols with aging and local marine aerosols). We believe that long-range transport aerosols significantly contributed to the increased accumulation mode particles as an external mixture in May. The accumulation mode particles were somewhat less hygroscopic and more volatile in September than in May. The additional exposure to a marine source due to ice melting may have led to a greater availability of biogenic compounds from the ocean, leading to the higher SF, while preferential wet removal of hygroscopic particles may have led to the lower HGF in September, although the number of particles was much smaller in September than in May. Detailed observation of the mixing structure of the accumulation particles indicated that an internal mixture of sulfate and volatile organics in the absence of nonvolatile cores was externally mixed with an internal mixture of sulfates and nonvolatile core species, such as sea salts, minerals, and soot. Occasionally, an elevated concentration of Aitken mode particles was observed at both sampling sites (Gruvbadet and Zeppelin) in May, which is believed to have been produced by nucleation. The Aitken mode particles displayed no significant external mixing. Biogenic compounds from the ocean may have contributed to the significant mass of the Aitken mode particles via nucleation. Analysis of the off-line TEM/EDS data also resulted in identification of the major types of submicrometer particles (<200–300 nm), i.e., organics, mixtures of organics and sulfates, soot, aged sea salts, and mineral dust particles. Sulfate and aged sea salts may have contributed to the particles with high HGF values, whereas the organics and mixture of organics and sulfate may have contributed to the volatile species. It is recommended that the mixing state, which was found to vary with size, air mass, and season, should be determined in the future to better understand the effects of Arctic aerosols on climate change (radiation balance and cloud formation).

■ ASSOCIATED CONTENT

📄 Supporting Information

Classification of air mass transport patterns (Siberia, northern Europe, northern Greenland, and the Arctic Ocean) in May, average mass concentration of submicrometer particles observed at the sampling site when the air mass passed over specific source regions in May and September 2012; TEM/EDS data related to possible organics, mixtures of organics and sulfate, soot, and aged sea salts; TEM/EDS data related to dust

particles (Si/Al/Fe/Ti/Ca) of various shapes (spherical, irregular, and rod-shaped). This material is available free of charge via the Internet at <http://pubs.acs.org>.

AUTHOR INFORMATION

Corresponding Author

*E-mail: kpark@gist.ac.kr. Tel: +82-62-715-3279. Fax: +82-62-715-2434.

Notes

The authors declare no competing financial interest.

ACKNOWLEDGMENTS

This research was supported by a National Research Foundation of Korea Grant funded by the Korean Government (NRF-C1ABA001-2011-0021064) and the National Leading Research Laboratory program funded by the National Research Foundation of Korea (NRF) grant (2011-0015548). Measurements at the Zeppelin station were supported by the Swedish Environmental Protection Agency (NV).

REFERENCES

- Behrenfeldt, U.; Krejci, R.; Ström, J.; Stohl, A. Chemical properties of Arctic aerosol particles collected at the Zeppelin station during the aerosol transition period in May and June of 2004. *Tellus, Ser. B* **2008**, *60 B* (3), 405–415.
- ACIA. *Arctic Climate Impact Assessment*; Cambridge, UK, 2005.
- Law, K. S.; Stohl, A. Arctic air pollution: Origins and impacts. *Science* **2007**, *315* (5818), 1537–1540.
- Shindell, D. T.; Faluvegi, G.; Koch, D. M.; Schmidt, G. A.; Linger, N.; Bauer, S. E. Improved attribution of climate forcing to emissions. *Science* **2009**, *326* (5953), 716–718.
- Hansen, J.; Nazarenko, L. Soot climate forcing via snow and ice albedos. *Proc. Natl. Acad. Sci., U. S. A.* **2004**, *101* (2), 423–428.
- Myhre, C. L.; Toledano, C.; Myhre, G.; Stebel, K.; Yttri, K. E.; Aaltonen, V.; Johnsrud, M.; Frioud, M.; Cachorro, V.; De Frutos, A.; Lihavainen, H.; Campbell, J. R.; Chaikovskiy, A. P.; Shiobara, M.; Welton, E. J.; Tørseth, K. Regional aerosol optical properties and radiative impact of the extreme smoke event in the European Arctic in spring 2006. *Atmos. Chem. Phys.* **2007**, *7* (22), 5899–5915.
- Eleftheriadis, K.; Vratolis, S.; Nyeki, S. Aerosol black carbon in the European Arctic: Measurements at Zeppelin station, Ny-Ålesund, Svalbard from 1998–2007. *Geophys. Res. Lett.* **2009**, *36* (2), No. 10.1029/2008GL035741.
- Koch, D.; Balkanski, Y.; Bauer, S. E.; Easter, R. C.; Ferrachat, S.; Ghan, S. J.; Hoose, C.; Iversen, T.; Kirkevåg, A.; Kristjansson, J. E.; Liu, X.; Lohmann, U.; Menon, S.; Quaas, J.; Schulz, M.; Seland, Ø.; Takemura, T.; Yan, N. Soot microphysical effects on liquid clouds, a multi-model investigation. *Atmos. Chem. Phys.* **2011**, *11* (3), 1051–1064.
- Serreze, M. C.; Barry, R. G. Processes and impacts of Arctic amplification: A research synthesis. *Global Planet. Change* **2011**, *77* (1–2), 85–96.
- Jacobson, M. Z. Strong radiative heating due to the mixing state of black carbon in atmospheric aerosols. *Nature* **2001**, *409* (6821), 695–697.
- Ramanathan, V.; Chung, C.; Kim, D.; Bettge, T.; Buja, L.; Kiehl, J. T.; Washington, W. M.; Fu, Q.; Sikka, D. R.; Wild, M. Atmospheric brown clouds: Impacts on South Asian climate and hydrological cycle. *Proc. Natl. Acad. Sci., U. S. A.* **2005**, *102* (15), 5326–5333.
- Ramanathan, V.; Ramana, M. V.; Roberts, G.; Kim, D.; Corrigan, C.; Chung, C.; Winker, D. Warming trends in Asia amplified by brown cloud solar absorption. *Nature* **2007**, *448* (7153), 575–578.
- IPCC. *Climate Change 2007: Synthesis Report*; Geneva, 2007
- Moffet, R. C.; Prather, K. A. In-situ measurements of the mixing state and optical properties of soot with implications for radiative

forcing estimates. *Proc. Natl. Acad. Sci., U. S. A.* **2009**, *106* (29), 11872–11877.

(15) Covert, D. S.; Heintzenberg, J. Size distributions and chemical properties of aerosol at Ny Alesund, Svalbard. *Atmos. Environ., Part A* **1993**, *27 A* (17–18), 2989–2997.

(16) Ström, J.; Umegård, J.; Tørseth, K.; Tunved, P.; Hansson, H. C.; Holmén, K.; Wismann, V.; Herber, A.; König-Langlo, G. One year of particle size distribution and aerosol chemical composition measurements at the Zeppelin Station, Svalbard, March 2000–March 2001. *Phys. Chem. Earth* **2003**, *28* (28–32), 1181–1190.

(17) Stohl, A. Characteristics of atmospheric transport into the Arctic troposphere. *J. Geophys. Res., D: Atmos.* **2006**, *111* (11), 16 DOI: 10.1029/2005JD006888.

(18) Quinn, P. K.; Shaw, G.; Andrews, E.; Dutton, E. G.; Ruoho-Airola, T.; Gong, S. L. Arctic haze: Current trends and knowledge gaps. *Tellus, Ser. B* **2007**, *59* (1), 99–114.

(19) Garrett, T. J.; Verzella, L. L. An evolving history of arctic aerosols. *Bull. Am. Meteorol. Soc.* **2008**, *89* (3), 299–302.

(20) Heintzenberg, J.; Leck, C. The summer aerosol in the central Arctic 1991–2008: Did it change or not? *Atmos. Chem. Phys.* **2012**, *12* (9), 3969–3983.

(21) Heintzenberg, J.; Larssen, S. SO₂ and sulfate in the arctic: Interpretation of observations at three Norwegian arctic-subarctic stations. *Tellus* **1983**, *35 B* (4), 255–265.

(22) Beine, H. J. Measurements of CO in the high Arctic. *Chemosphere: Global Change Sci.* **1999**, *1* (1–3), 145–151.

(23) Sirois, A.; Barrie, L. A. Arctic lower tropospheric aerosol trends and composition at Alert, Canada: 1980–1995. *J. Geophys. Res. D: Atmos.* **1999**, *104* (D9), 11599–11618.

(24) Quinn, P. K.; Miller, T. L.; Bates, T. S.; Ogren, J. A.; Andrews, E.; Shaw, G. E. A 3-year record of simultaneously measured aerosol chemical and optical properties at Barrow, Alaska. *J. Geophys. Res. D: Atmos.* **2002**, *107* (11), AAC 8-1–AAC 8-15.

(25) Hirdman, D.; Burkhardt, J. F.; Sodemann, H.; Eckhardt, S.; Jefferson, A.; Quinn, P. K.; Sharma, S.; Ström, J.; Stohl, A. Long-term trends of black carbon and sulphate aerosol in the Arctic: Changes in atmospheric transport and source region emissions. *Atmos. Chem. Phys.* **2010**, *10* (19), 9351–9368.

(26) Frossard, A. A.; Shaw, P. M.; Russell, L. M.; Kroll, J. H.; Canagaratna, M. R.; Worsnop, D. R.; Quinn, P. K.; Bates, T. S. Springtime Arctic haze contributions of submicron organic particles from European and Asian combustion sources. *J. Geophys. Res. D: Atmos.* **2011**, *116* (5), No. 10.1029/2010jd015178.

(27) Shantz, N. C.; Gultepe, I.; Liu, P. S. K.; Earle, M. E.; Zelenyuk, A. Spatial and temporal variability of aerosol particles in Arctic spring. *Q. J. R. Meteorol. Soc.* **2012**, *138* (669), 2229–2240.

(28) Weinbruch, S.; Wiesemann, D.; Ebert, M.; Schütze, K.; Kallenborn, R.; Ström, J. Chemical composition and sources of aerosol particles at Zeppelin Mountain (Ny Ålesund, Svalbard): An electron microscopy study. *Atmos. Environ.* **2012**, *49*, 142–150.

(29) Engvall, A. C.; Krejci, K.; Ström, J.; Treffeisen, R.; Scheele, R. Changes in aerosol properties during spring-summer period in the Arctic troposphere. *Atmos. Chem. Phys. Discuss.* **2007**, *7*, 1215–1260.

(30) Engvall, A. C.; Krejci, R.; Ström, J.; Treffeisen, R.; Scheele, R.; Hermansen, O.; Paatero, J. Changes in aerosol properties during spring-summer period in the Arctic troposphere. *Atmos. Chem. Phys.* **2008**, *8* (3), 445–462.

(31) Ström, J.; Engvall, A. C.; Delbart, F.; Krejci, R.; Treffeisen, R. On small particles in the Arctic summer boundary layer: Observations at two different heights near Ny-Ålesund, Svalbard. *Tellus, Ser. B* **2009**, *61 B* (2), 473–482.

(32) Shaw, G. E. The Arctic haze phenomenon. *Bull. Am. Meteorol. Soc.* **1995**, *76* (12), 2403–2413.

(33) Lavoué, D.; Lioussé, C.; Cachier, H.; Stocks, B. J.; Goldammer, J. G. Modeling of carbonaceous particles emitted by boreal and temperate wildfires at northern latitudes. *J. Geophys. Res. D: Atmos.* **2000**, *105* (D22), 26871–26890.

(34) Browse, J.; Carslaw, K. S.; Arnold, S. R.; Pringle, K.; Boucher, O. The scavenging processes controlling the seasonal cycle in Arctic

sulphate and black carbon aerosol. *Atmos. Chem. Phys.* **2012**, *12* (15), 6775–6798.

(35) Nishita, C.; Osada, K.; Hara, K.; Kido, M.; Wada, M.; Shibata, T.; Iwasaka, Y. Number-size distributions of atmospheric aerosol particles (10–365 μm) at Ny-Alesund, Norwegian arctic: Their relationship with air mass history. *Polar Meteorol. Glaciol.* **2001**, *15*, 67–77.

(36) Zábory, J.; Matisans, M.; Krejci, R.; Nilsson, E. D.; Ström, J. Artificial primary marine aerosol production: A laboratory study with varying water temperature, salinity, and succinic acid concentration. *Atmos. Chem. Phys.* **2012**, *12* (22), 10709–10724.

(37) Tunved, P.; Ström, J.; Krejci, R. Arctic aerosol life cycle: Linking aerosol size distributions observed between 2000 and 2010 with air mass transport and precipitation at Zeppelin station, Ny-Ålesund, Svalbard. *Atmos. Chem. Phys.* **2013**, *13* (7), 3643–3660.

(38) Rader, D. J.; McMurry, P. H. Application of the tandem differential mobility analyzer to studies of droplet growth or evaporation. *J. Aerosol Sci.* **1986**, *17* (5), 771–787.

(39) Park, K.; Kim, J. S.; Miller, A. L. A study on effects of size and structure on hygroscopicity of nanoparticles using a tandem differential mobility analyzer and TEM. *J. Nanopart. Res.* **2009**, *11* (1), 175–183.

(40) Park, K.; Kim, J. S.; Park, S. H. Measurements of hygroscopicity and volatility of atmospheric ultrafine particles during ultrafine particle formation events at urban, industrial, and coastal sites. *Environ. Sci. Technol.* **2009**, *43* (17), 6710–6716.

(41) Quennehen, B.; Schwarzenboeck, A.; Matsuki, A.; Burkhart, J. F.; Stohl, A.; Ancellet, G.; Law, K. S. Anthropogenic and forest fire pollution aerosol transported to the Arctic: Observations from the POLARCAT-France spring campaign. *Atmos. Chem. Phys.* **2012**, *12* (14), 6437–6454.

(42) Leek, C.; Bigg, E. K. Aerosol production over remote marine areas - A new route. *Geophys. Res. Lett.* **1999**, *26* (23), 3577–3580.

(43) Wiedensohler, A.; Covert, D. S.; Swietlicki, E.; Aalto, P.; Heintzenberg, J.; Leck, C. Occurrence of an ultrafine particle mode less than 20 nm in diameter in the marine boundary layer during Arctic summer and autumn. *Tellus, Ser. B* **1996**, *48* (2), 213–222.

(44) O'Dowd, C. D.; Smith, M. H.; Consterdine, I. E.; Lowe, J. A. Marine aerosol, sea-salt, and the marine sulphur cycle: A short review. *Atmos. Environ.* **1997**, *31* (1), 73–80.

(45) O'Dowd, C. D.; Facchini, M. C.; Cavalli, F.; Ceburnis, D.; Mircea, M.; Decesari, S.; Fuzzi, S.; Young, J. Y.; Putaud, J. P. Biogenically driven organic contribution to marine aerosol. *Nature* **2004**, *431* (7009), 676–680.

(46) Hara, K.; Yamagata, S.; Yamanouchi, T.; Saton, K.; Herber, A.; Iwasaka, Y.; Nagatani, M.; Nakata, H. Mixing states of individual aerosol particles in spring Arctic troposphere during ASTAR 2000 campaign. *J. Geophys. Res. D: Atmos.* **2003**, *108* (7), AAC 2-1–AAC 2-12.

(47) Eneroth, K.; Kjellström, E.; Holmén, K. A trajectory climatology for Svalbard; Investigating how atmospheric flow patterns influence observed tracer concentrations. *Phys. Chem. Earth* **2003**, *28* (28–32), 1191–1203.

(48) Kahl, J. D. W.; Martinez, D. A.; Zaitseva, N. A. Long-term variability in the low-level inversion layer over the Arctic Ocean. *Int. J. Climatol.* **1996**, *16* (11), 1297–1313.